

**ADVANCED
MATERIALS
TECHNOLOGIES**

Supporting Information

for *Adv. Mater. Technol.*, DOI: 10.1002/admt.201700136

Batch Fabrication of Customizable Silicone-Textile
Composite Capacitive Strain Sensors for Human Motion
Tracking

*Asli Atalay, Vanessa Sanchez, Ozgur Atalay, Daniel M. Vogt,
Florian Haufe, Robert J. Wood, and Conor J. Walsh**

Supporting Information

Title: Batch Fabrication of Customizable Silicone-Textile Composite Capacitive Strain Sensors for Human Motion Tracking

Asli Atalay, Vanessa Sanchez, Ozgur Atalay, Daniel Vogt, Florian Haufe, Robert J. Wood, Conor J. Walsh

Supporting Experimental Section

Attaching Handles and Sensor Encapsulation: Using Fabri-Tac Permanent Adhesive (Beacon Adhesives, Inc., USA), woven textile (Typhoon Wide DWR - 00552v, Milliken, USA) reinforcement handles are adhered to sensor with 7.5 mm overlap and set at room temperature for 24 hrs. Un-encapsulated sensors are complete at this stage.

For encapsulated sensors, silicone is prepared using Ecoflex 0030 with a 1:1 ratio of Part A and Part B and adding 10 wt% NOVOCS Gloss silicone solvent (both obtained from Smooth-On Inc.) for ease of pouring, mixing in the centrifugal planetary mixer with the same method as dielectric material production. Dogbone molds of the dimensions specified in the ASTM D412 standard are 3D printed from VeroBlue (RGD840), a photo-curable acrylate resin on an Objet30 3D printer (Stratasys, Eden Prairie, MN, USA). Sensors with handles are placed into the molds, raising incorporated connection leads above the liquid level using wire and masking tape. 4 g of prepared silicone is poured on top of each sensor. The entire mold is degassed under vacuum for 3 min and transferred to an oven to cure at 70 °C for 20 min.

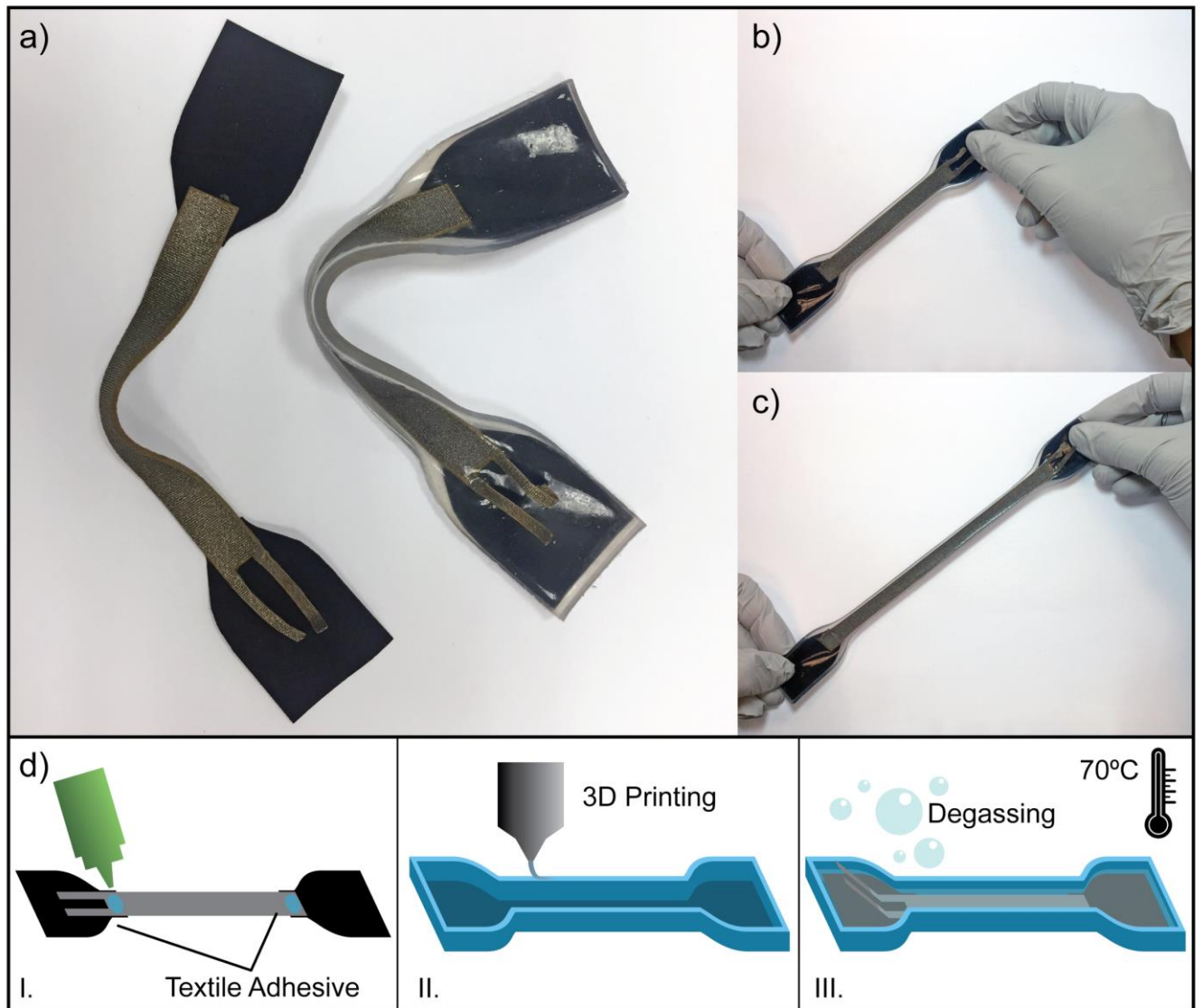


Figure S1. a) Image of plain and encapsulated sensor with attached handles. b) Encapsulated sensor at 0% strain. c) Encapsulated sensor at approximately 100% strain. d) Attachment of handles and sensor encapsulation: i. Affixing handles with fabric adhesive. ii. 3D printing of ASTM D412 mold. iii. Degassing and curing the silicone poured on top of the sensor.

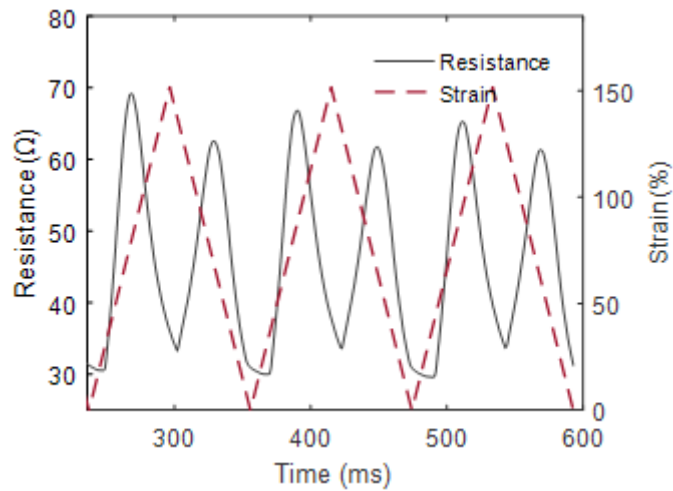
Resistance change of the Fabric electrodes

Figure S2. Conductive fabric electrode resistance change as a function of applied strain from 0% to 150%.

Dynamic characterization of resistance change of fabric electrodes has been conducted on an electromechanical tester (Instron 5544A). Resistance and extension data were recorded. The resistance change of a plain fabric electrode was determined by stretching the samples for five cycles from 0% to 150% strain at a crosshead speed of 8 mm/s. The prepared sample's dimensions were 10 x 80 mm. The resistance change range of a fabric electrode at 0% - 150% strain is between 30 - 75 Ω for these sensor dimensions.

We calculated the time constant for the sensor to charge/discharge to be on the order of several nanoseconds.

Materials and sensor geometry after uniaxial stretching

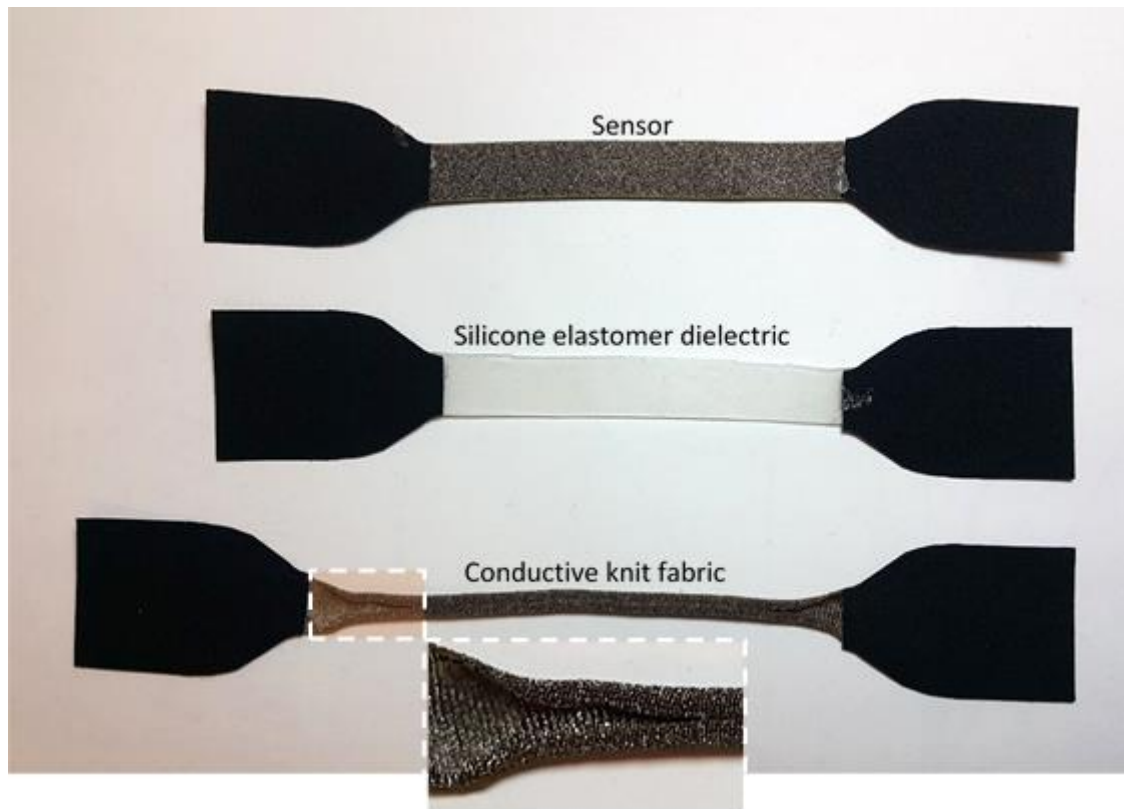


Figure S3. Dimensional stability of the sensor, silicone, and conductive fabric after being stretched to 150% and released. Inset showing the typical rolling behavior of knit fabric after being stretched and released.

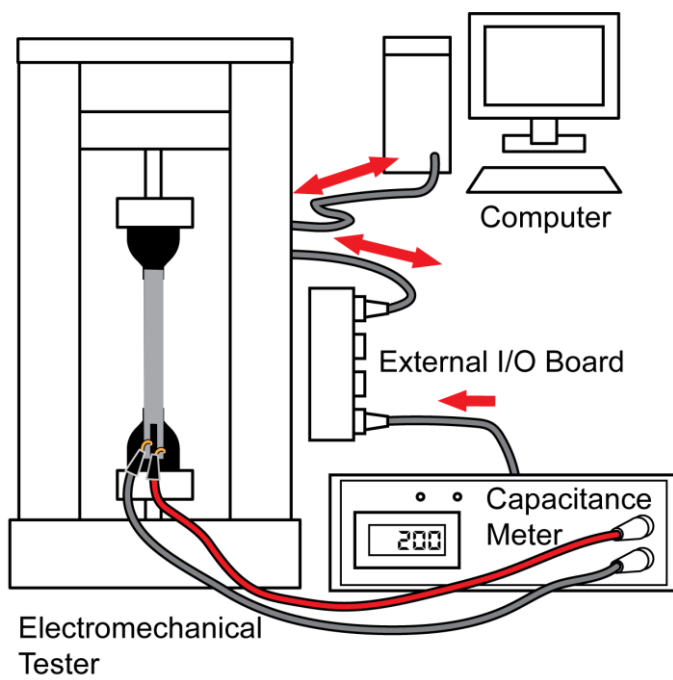
Electromechanical test set-up

Figure S4. Experimental test setup to synchronously obtain mechanical data and electrical signal output of the sensor. A commercial electromechanical tester (Instron 5544A) and a capacitance meter (Model 3000, GLK Instruments CA, USA) were connected via a common I/O interface, (BNC-2111, National Instruments Corp.) and extension, load, and capacitance data are logged.

*Effect of dielectric thickness of the sensor on sensor linearity and GF***Table S1.** Gauge factor and linearity values of the sensors manufactured at different dielectric thicknesses

Dielectric T	Gauge Fact	Lin
102 μm	0.601 \pm 0.005	0.9
187 μm	0.989 \pm 0.004	0.9
335 μm	1.033 \pm 0.002	0.9
500 μm	1.229 \pm 0.004	0.9
710 μm	1.033 \pm 0.004	0.9

Characterization of the dielectric thickness effect of sensors was conducted on an electromechanical tester (Instron 5544A). Samples were prepared at discrete dielectric thicknesses of 102, 187, 335, 500, 710 μm with dimensions of 10mm x 80mm. Five samples were tested from each group. As seen from Table S1, gauge factor and linearity values of the samples within the same group exhibited negligible difference and this could be attributed to batch manufacturing process which creates sensors with consistent properties. Each sensor was preconditioned by applying 20 cycles before testing. Samples were uniaxially stretched up to 100% strain at a speed of 24mm/s for 20 cycles. The sensors with thicker dielectric layers (187, 335, 500, 710, μm) showed highly elastic behavior up to 100% strain with high linearity, increased GF, and negligible hysteresis. However, the sensor sample with the thinnest dielectric (102 μm) presented a significant viscoelastic creep resulting in increased relaxation time after an applied tensile strain. This behavior is due to dominating viscoelastic properties of conductive fabric electrodes, resulting from the lack of dielectric material with good elasticity. Mannsfeld et al. also explain this phenomenon for pressure sensing capacitive

sensors i.e., thin PDMS film dielectrics (few micrometers) exhibit viscoelastic creep due to irreversible entanglement of polymer chains and lack of deformable surfaces resulting in inability to displace material to an applied load. ^[1] Although this phenomena is described for compressive strain, this explanation could be applicable for tensile strain as well.

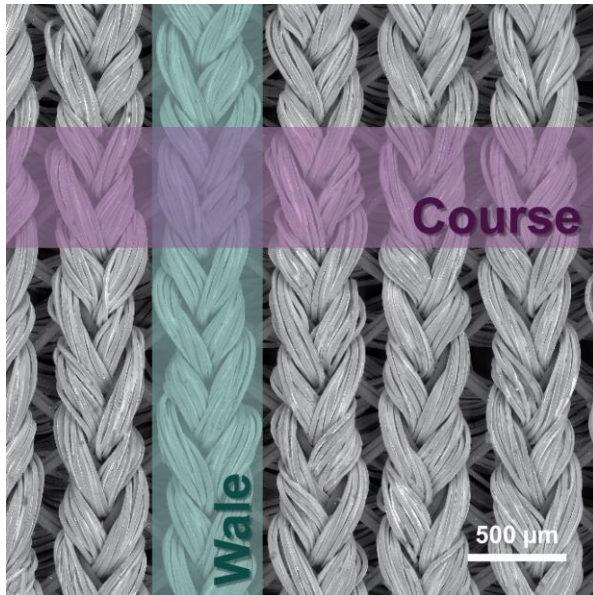


Figure S5. Wale and Course directions as seen on face (dull side) of electrode fabric structure. In this textile, the direction parallel to the wale structure has a lower modulus, causing sensors to be cut with their stretchable length parallel to this direction.

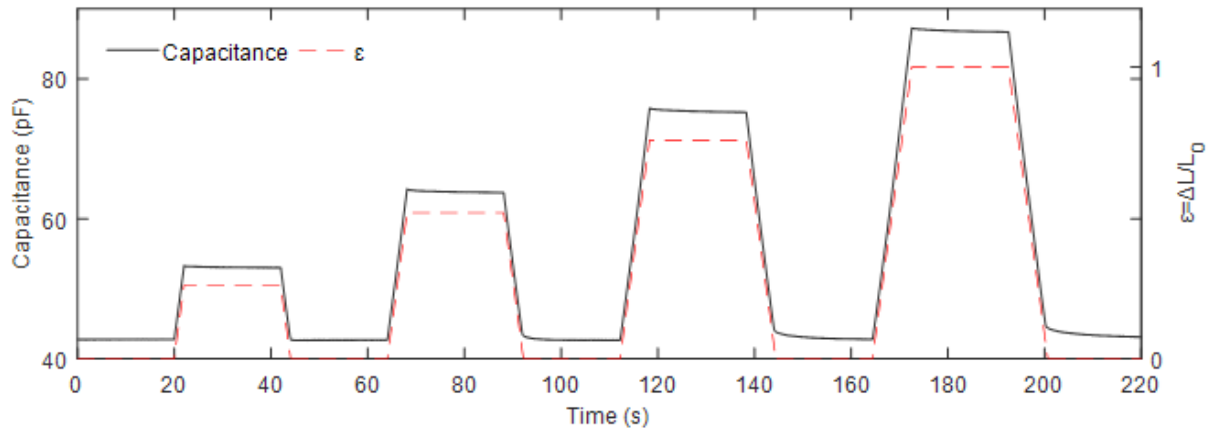
Drift of the sensor under static loading

Figure S6. Static drift of the sensor under constant strain levels at $\epsilon=0.25, 0.5, 0.75, 1.0$ holding for 20 seconds.

As shown in Figure S6, $\epsilon=0.25, 0.50, 0.75$ and 0.1 levels of strain were applied to the capacitive sensor at a strain ramping rate of 8mm/s and kept for 20 seconds at these strain levels in order to observe the drift characteristics of the sensor under static loading. Drift error was calculated as the change in the sensor capacitance response to a constant strain value. The drift of the capacitance values of the strain sensor to be found to be 0.3% , 0.7% , 0.6% and 0.5% for the strain levels of $\epsilon=0.25, 0.50, 0.75$ and 0.1 , respectively.

Sensor Resolution

Sensor resolution has been assessed based on electrical signal noise levels at 0%, 25 %, 50 %, 75% and 100 % strain. All measurements were obtained while maintaining the full sensing bandwidth of approximately 40 Hz. The resolution values correspond to a 95% confidence interval around the measured value, or 4 sigma.

Table S2. Calculated resolution values of the sensor at different strain levels

Strain Level	Absolute Resolution	Relative Resolution
0%	0.4% (MDS = 0.2 %)	n/a
25%	0.54%	2.16%
50%	0.98%	1.96%
75%	1.21%	1.61%
100%	1.24%	1.24%

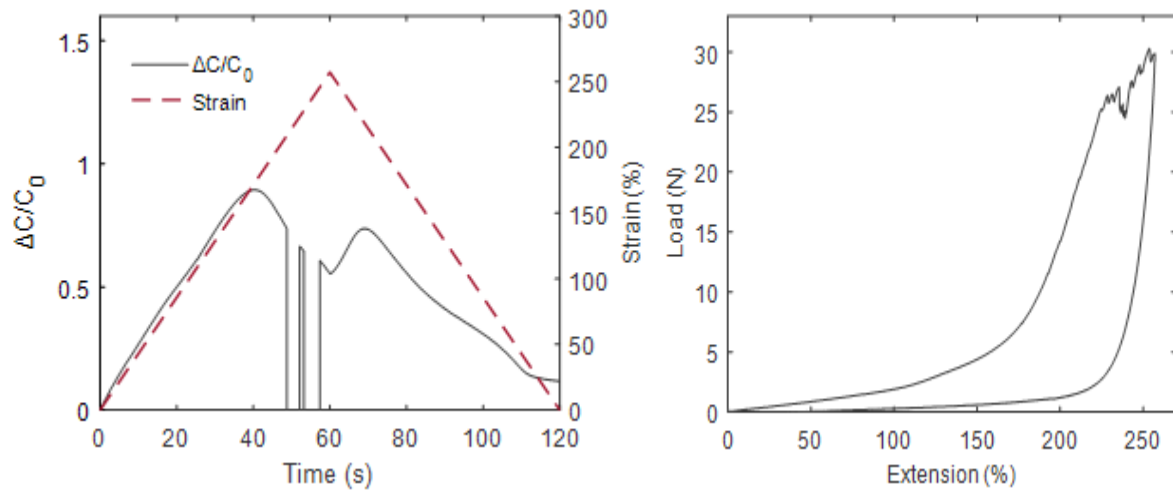
Electromechanical failure test

Figure S7. Electromechanical failure test. a) Relative capacitance change is represented by the grey line and percent strain change is represented by a dotted red line as a function of time. b) Load change as a function of strain.

An electromechanical failure test was conducted by stretching the sensor up to 250% at a speed of 3 mm/s. Signal was lost at 170% strain and permanent deformation occurred on the sensor elasticity and the handle joints at 220% strain as shown in Figure S7.

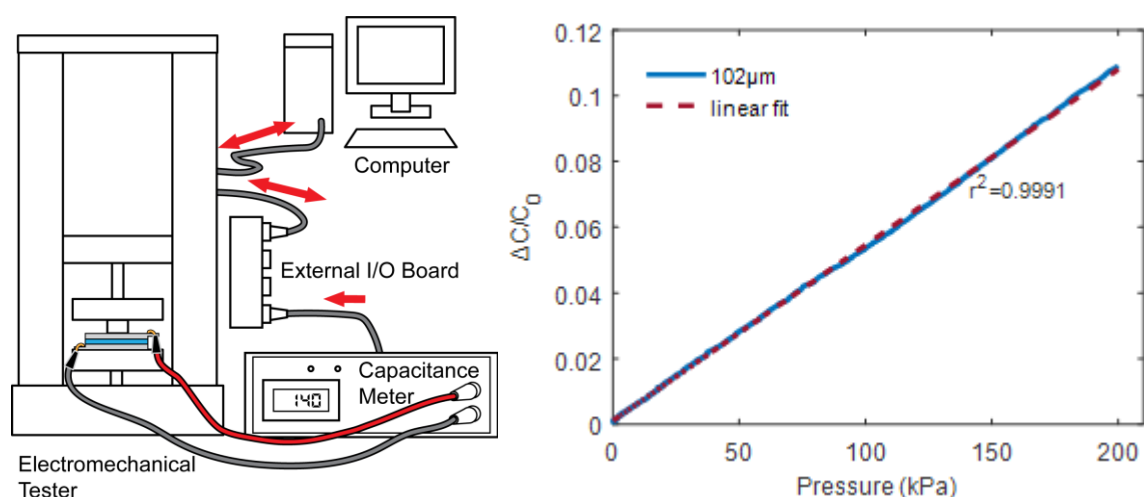
Pressure test

Figure S8. Normal pressure test. a) Test setup to synchronously obtain pressure data and electrical signal output of the sensor. b) Relative capacitance change as a function of pressure.

Dynamic characterization of the pressure was conducted on the sensor with the thinnest achievable dielectric layer, 102 μm . When we increased the dielectric thickness, sensitivity and linearity of the sensors decreased proportionally. The sample was placed between the pressure platens of the Instron. A sensor area of 1cm^2 was pressurized at a speed of 0.1 mm/s. Figure S8a presents a linear response to pressure up to 200 kPa with an r^2 value of 0.9991. The Gauge Factor for pressure is calculated as $5.45 \times 10^{-4} \text{ kPa}^{-1}$.

References

- [1] S. C. Mannsfeld, B. C. Tee, R. M. Stoltenberg, C. V. H. Chen, S. Barman, B. V. Muir, A. N. Sokolov, C. Reese, Z. Bao, *Nature materials* 2010, 9, 859